Available online at www.sciencedirect.com
ScienceDirect
Earth and Planetary Science Letters 249 (2006) 290–306
EPSL
www.elsevier.com/locate/epsl

Mechanisms controlling the silicon isotopic compositions of river waters

R.B. Georg [a,*], B.C. Reynolds [a], M. Frank [b], A.N. Halliday [c]

[a] ETH Zürich, Institute for Isotope Geochemistry and Mineral Resources, ETH Zentrum, Sonneggstrasse 5, CH-8092 Zürich, Switzerland
[b] IfM-GEOMAR, Leibniz Institute for Marine Sciences, Wischhofstrasse 1-3, D-24148 Kiel, Germany
[c] University of Oxford, Department of Earth Sciences, Parks Road, OX 3PR Oxford, UK

Received 22 March 2006; received in revised form 29 June 2006; accepted 6 July 2006
Available online 23 August 2006
Editor: H. Elderfield

Abstract

It has been proposed that silicon (Si) isotopes are fractionated during weathering and biological activity leading to heavy dissolved riverine compositions. In this study, the first seasonal variations of stable isotope compositions of dissolved riverine Si are reported and compared with concomitant changes in water chemistry. Four different rivers in Switzerland were sampled between March 2004 and July 2005. The unique high-resolution multi-collector ICP-MS Nu1700, has been used to provide simultaneous interference-free measurements of ^{28}Si, ^{29}Si and ^{30}Si abundances with an average limiting precision of ±0.04‰ on δ^{30}Si. This precision facilitates the clarification of small temporal variations in isotope composition. The average of all the data for the 40 samples is δ^{30}Si=+0.84±0.19‰ (±1σ_{SD}). Despite significant differences in catchment lithologies, biomass, climate, total dissolved solids and weathering fluxes the averaged isotopic composition of dissolved Si in each river is strikingly similar with means of +0.70±0.12‰ for the Birs,+0.95±0.22‰ for the Saane,+0.93±0.12‰ for the Ticino and +0.79±0.19‰ for the Verzasca. However, the δ^{30}Si undergoes seasonal variations of up to 0.6‰. Comparisons between δ^{30}Si and physico–chemical parameters, such as the concentration of dissolved Si and other cations, the discharge of the rivers, and the resulting weathering fluxes, permits an understanding of the processes that control the Si budget and the fate of dissolved Si within these rivers.

The main mechanism controlling the Si isotope composition of the mountainous Verzasca River appears to be a two component mixing between the seepage of soil/ground waters, with heavier Si produced by clay formation and superficial runoff associated with lighter Si during high discharge events. A biologically-mediated fractionation can be excluded in this particular river system. The other rivers display increasing complexity with increases in the proportion of forested and cultivated landscapes as well as carbonate rocks in the catchment. In these instances it is impossible to resolve the extent of the isotopic fractionation and contributed flux of Si contributed by biological processes as opposed to abiotic weathering.

The presence of seasonal variations in Si isotope composition in mountainous rivers provides evidence that extreme changes in climate affect the overall composition of dissolved Si delivered to the oceans. The oceanic Si isotope composition is very sensitive to even small changes in the riverine Si isotope composition and this parameter appears to be more critical than

* Corresponding author. Tel.: +41 1 63 20730; fax: +41 1 63 21179.
E-mail address: georg@erdw.ethz.ch (R.B. Georg).

doi:10.1016/j.epsl.2006.07.006

plausible changes in the Si flux. Therefore, concurrent changes in weathering style may need to be considered when using the Si isotopic compositions of diatoms, sponges and radiolaria as paleoproductivity proxies.

Keywords: Si isotopes; seasonal variability; river; weathering; MC-ICPMS

1. Introduction

Weathering of silicate minerals and rocks is a fundamental process that is thought to regulate global climate on long timescales as a result of the drawdown of atmospheric CO_2 [1–4]. During breakdown of silicate minerals chemical weathering consumes CO_2 and contributes species such as silicon (Si) to the dissolved load of rivers [5]. In order to model long-term weathering and CO_2 consumption, different approaches have been applied, such as mass balance calculations using major and minor elemental fluxes of rivers [6–8], and radiogenic and stable isotope proxies, such as strontium [9] and lithium [10,11]. Despite being a major constituent of silicate minerals and the continental crust, Si is usually excluded from calculations of chemical weathering fluxes owing to the complication of biogenic silica formation [8]. Silicon is released by weathering of silicate rocks and minerals and can be recycled by biological processes in soils before it finally reaches the rivers and leaves the catchments [12–14]. Silicon isotopes should in principle provide a constraint on the origin and mass budget of riverine dissolved Si. Detailed investigations on riverine Si isotope compositions have not yet been undertaken, but are now tractable using MC-ICPMS analyses [15].

It has been shown that rivers contain Si that is isotopically heavy relative to the continental crust [16,17]. In principle two fractionation processes can explain the observed heavy isotope compositions of dissolved Si in rivers: (i) weathering of igneous minerals, and (ii) biological utilisation of resulting silicic acid. Secondary clays are isotopically lighter and balanced by a corresponding enrichment of heavy Si in ambient fluids [17–21]. Organisms incorporate Si from ambient fluids and form biogenic silica, e.g. skeletal material (diatoms) and phytoliths (higher land plants). Various studies have shown that during the formation of biogenic silica organisms discriminate against heavier Si isotopes, resulting in a lighter isotope composition of biogenic silica and a corresponding enrichment of heavier Si isotopes in coexisting ambient solutions [22–28]. Therefore, both biogenic processes and weathering can generate heavy dissolved Si in river waters. In principle, both can affect the composition of Si in seawater, yet this is assumed to be constant when inferring paleoproductivity from diatom records [23].

Little is known about the mechanisms controlling the Si isotope composition in rivers under different climatic conditions. In order to understand this and the role of biological processes versus weathering it is necessary to investigate whether the Si isotope composition of particular river systems varies with seasonality, weathering rates and lithology. To investigate the role of catchment lithology and relief, four rivers draining three different parts of the Swiss Alps have been sampled; the Birs in the north, the Saane in central Switzerland and the Verzasca and Ticino in the south. These rivers were sampled over an annual cycle, from March 2004 to July 2005. The concentration (or [Si]) and isotopic composition of dissolved Si were measured and compared with the cation composition in order to constrain the geochemistry of Si within these different catchments. A comparison of the Si isotope composition with physico–chemical parameters, such as river discharge, the water chemistry and the resulting weathering flux can help to constrain the processes that control the Si isotope composition of these catchments. A positive correlation between Si isotope composition and concentration of riverine Si was first recognised by De la Rocha et al. (2000) and interpreted as the result of enhanced weathering (higher δ^{30}Si and higher [Si]) [17]. Biological processes in contrast remove Si from solution and therefore generate a negative correlation between isotopic composition and concentration of dissolved Si. Such a model may however be too simplistic, as explored in this paper.

2. Sampling and analytical methods

2.1. Sampling sites and geological setting

The location of the sampling sites and respective catchment areas are shown in Fig. 1; some details on the geomorphology are given in Table 1. The Verzasca and the Ticino rivers are both located in the Tessin, and drain catchments dominated by the lithology of the Pennine units of the central Alps. The bedrocks are predominantly crystalline gneisses with some calcareous shists (Bündnerschiefer) and evaporites in the north of the

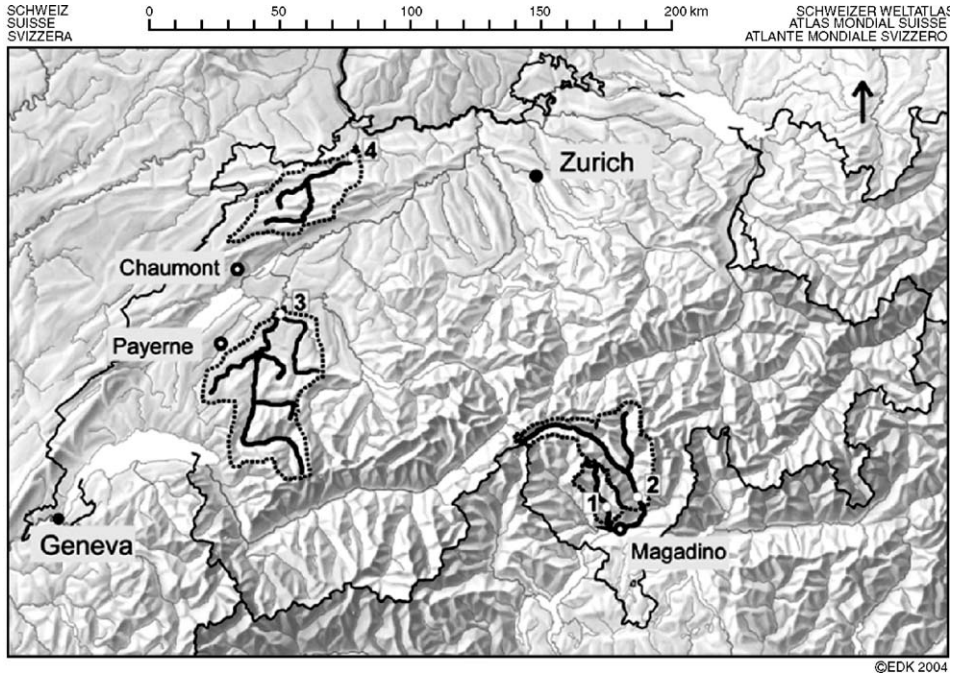

Fig. 1. Map of Switzerland showing the four sample stations (white dots), the river courses (black lines) and catchment outlines (black pointed lines). Station 1 = Verzasca, Station 2 = Ticino, Station 3 = Saane, Station 4 = Birs. Rainwater composition was taken at stations in Chaumont, Payerne and Magadino (open black cycles).

Ticino catchment [29]. The Verzasca is a high mountain river with small catchment (186 km^2) that has eroded a narrow V-shaped valley into the crystalline bedrock. Bedrock outcrops and thin soil layers dominate the catchment's surface. In the Ticino catchment (1515 km^2) the main valley consists of cultivated alluvial flood plains covered with extensive soil horizons, flanked on both sides by high mountains. The two other rivers, the Birs (catchment size of 911 km^2) and the Saane (catchment size of 1861 km^2), are located within the Helvetic unit of the Alps and represent meandering river systems. The land use in both catchments is mainly agriculture and forestry. The Birs is located in the northern part of Switzerland and mainly drains the Swiss Jura Mountains, where shallow marine carbonate deposits dominate over minor proportions of siliciclastic sediments. The catchment of the Saane covers a variety of different sedimentary lithologies, mainly marine siliciclastic rocks (Flysch and Molasse), but also carbonate-sandstones, mudstones and limestones.

2.2. Sampling

Each of the four rivers was sampled 10 times during 2004 and 2005. Sample locations were chosen to be near monitoring stations of the Swiss Federal Office for the Environment (FOEN), so that changes in discharge for each sampling point are well documented (Fig. 1). River water samples were filtered directly at the sampling site through 0.45 μm Millipore cellulose acetate filters and acidified with suprapure HCl to a pH between 2 and 3. The [Si] was measured colometrically by the molybdenum blue method using a spectrophotometer at the laboratory at ETH Zürich 1 d later [30]. Cation concentration measurements for each sample were performed by ICP-MS at ACME Analytical Laboratories Ltd. in Vancouver, Canada.

2.3. Source of additional data

The hydrochemical parameters of Saane, Birs and Ticino were part of a long-term investigation of the NADUF (National programme for the long-term analytical investigation of Swiss rivers) monitoring program, in collaboration with the Swiss Federal Institute of Aquatic Science and Technology (EAWAG) [31]. The NADUF program provides a database for hydrochemical data, such as pH, temperature, major cation and anion composition, and covers periods beginning in 1978 to the late 1990s. The Verzasca has been monitored as part of an international program

Table 1
Long-term average chemistry data of the studied rivers

River	Station	AVE catchment		Discharge (m^3/s)	Temp (°C)	pH	$HCO3^-$	$SO42^-$	$NO3^-$	Cl^-	$Ca2^+$	$Mg2^+$	Na^+	K^+	Si	Σ^- (meq/l)	Σ^+ (meq/l)	TDS (mg/l)
	Alt. a.s.l.	Elevation	Slope				(mg/l)											
Average long-term data (additional sources, see Section 2.3), uncorrected for wet depositional input																		
Birs	268 m	740 m	14.5°	15	10.7	8.2*	257.1	22.5	12.5	11.0	90.0	4.4	7.2	2.3	2.2	5.21	5.24	409.2
Saane	474 m	1130 m	16.3°	57	9.7	8.2	199.9	34.6	6.6	6.3	69.4	7.6	4.6	1.6	1.9	4.28	4.32	332.5
Ticino	250 m	1640 m	29.8°	75	8.9	7.8	60.1	62.1	3.3	2.2	36.2	5.7	2.4	1.9	2.4	2.40	2.44	175.8
Verzasca	550 m	1574 m	29.5°	12	7.0	6.7	3.6	3.6	3.1	0.3	2.6	0.2	0.7	0.5	1.8	0.20	0.19	16.4

Station		Precipitation (mm)	pH	SO_4^{2-}	NO^{3-}	Cl^-	Ca^{2+}	Mg^{2+}	Na^+	K^+
Annual average chemical composition of rain waters in mg/l										
Magadino	(Ticino, Verzasca)	1649	5.1	1.4	2.4	0.23	0.41	0.05	0.15	0.05
Payerne	(Saane)	869	5.3	0.87	1.3	0.18	0.31	0.03	0.11	0.05
Chaumont	(Birs)	1101	5.2	0.72	1.06	0.21	0.22	0.03	0.12	0.03
Annual average rain water element fluxes in mg/m²/year										
Magadino	(Ticino, Verzasca)			2324	3948	384	678	78	241	76
Payerne	(Saane)			745	1155	156	267	26	98	47
Chaumont	(Birs)			802	1150	231	239	30	134	37
Correction factors for wet depositional input in %										
Birs				6.7	17.4	4.0	0.5	1.3	3.4	3.1
Saane				2.3	18.3	2.6	0.4	0.4	2.2	3.0
Ticino				2.4	76.0	11.2	1.2	0.9	6.5	2.6
Verzasca				31	61	63	13.2	17.3	16.7	7.0

The annual average composition of rainwater is used to calculate correction factors for wet depositional input. *pH value of the Birs is based on field measurements throughout 2004–2005.

(Cooperative Programme on Assessment and Monitoring of Acidification of Rivers and Lakes: ICP-waters), which has been established by the United Nations Economic Commission for Europe's Convention on Long-Range Transboundary Air Pollution (LRTAP). We used these long-term datasets to constrain the basic water chemistry of the investigated rivers.

The chemical composition of rainwater was taken from the NABEL (National Air Pollution Monitoring Network) program [32]. We have chosen three stations that are close to the studied catchments. The selected stations are Magadino (for Ticino and Verzasca), Payerne (for Saane) and Chaumont (for Birs) (Fig. 1). Annual average rainwater compositions are provided as concentration (mg/l) and as elemental flux (mg/m^2/yr) for the year 2004 (Table 1). The rainwater compositions and the long-term chemistry data were used to calculate correction factors for wet depositional input, which were then applied to the cation composition of the river water samples in order to obtain weathering-derived dissolved fluxes.

2.4. Correction for wet depositional input

In order to correct the dissolved riverine load for wet depositional contributions correction factors were calculated in two ways: First using the Cl^- based method [33] and second using a volumetric approach comparing the wet depositional element flux per unit area per year with the riverine flux of the specific element. The Cl^- correction yields negative riverine fluxes of NO_3^- and SO_4^{2-} for the Birs and Saane and negative riverine fluxes of NO_3^- for the Ticino. These negative fluxes show that the Cl^- load of these three rivers cannot only have been of atmospheric origin but that there must have been an additional input that probably originated from road salt and fertilizers. The volumetric approach uses the elemental flux in precipitation compared with the average annual riverine amount of the element dissolved. The correction factor represents the percentage of the rainwater contribution to the specific riverine element annual flux. This approach is not able to reconcile the high NO_3^- flux observed in the Verzasca. Both correction approaches are subject to errors as average rain compositions and precipitation data are deployed. In addition, the rainwater compositions were not directly measured within the catchment introducing possible geographical biases. The volumetric approach yields more consistent data so these correction factors were used to correct for wet depositional input (Table 1). No data exist for the Si concentrations of these rainwater pools, but the Si concentration of rain is usually very low, especially when compared to cation concentrations [33,34]. Therefore, the Si contribution from rain is assumed to be insignificant compared to weathering Si fluxes.

2.5. Chemical preparation techniques

Silicon was separated from the water matrix and purified using a newly developed cation-exchange chemistry [35]. All acids used were distilled by sub-boiling in Savillex elbows. Dilutions used deionised water (MilliQ-element "MQ-e" (Millipore)). The Si blank in the reagents is below the detection limit (1 ppb) of the Molybdate-blue method using a spectrophotometer.

The new ion-exchange chromatographic separation and purification technique for Si is based on a cation-exchange process, whereby Si is separated from the entire cation matrix of the sample using ion exchange columns filled with a resin bed of 1.8 ml DOWEX 50W-X12 (200–400 mesh). The ion-chromatography separates 3.6 μg Si from the cationic species and the purified sample solutions were diluted to 0.6 mg/l Si (21 μM) for mass spectrometric measurement. The Si recovery for the separation procedure is 100% and no column induced Si isotope fractionation has been found using standard solutions. The eluted sample is effectively free of all cationic species including trace metals [35].

2.6. Mass spectrometry

The direct measurement of Si isotopes by MC-ICPMS requires high-resolution mass-spectrometry in order to resolve Si^+ ions from polyatomic interferences of similar mass, in particular $^{14}N^{16}O^+$ interferences on the $^{30}Si^+$ ion beam [36,37]. We have analysed Si isotopes using the high-resolution capacity of the Nu1700 (Nu Instruments, UK) multiple collector-ICPMS at ETH Zürich [15]. A true high mass resolution of 2000 (m/Δm at 10% peak valley) allows for a separation of the three Si^+ ion beams from all major polyatomic interferences including $^{12}C^{16}O^+$, $^{14}N^{14}N^+$, $^{14}N^{15}N^+$, $^{14}N^{14}N^1H^+$ and $^{14}N^{16}O^+$. Samples are introduced to the plasma via a DSN-100 desolvating nebuliser system (Nu Instruments, UK) using a 6 mm PFA nebuliser (Elemental Scientific Inc.) with a variable uptake rate of between 60 and 80 μl/min. All three Si peaks are measured simultaneously in static mode with Faraday collectors equipped with

10^{11} Ω resistors. The mass bias of the Nu1700 is very stable with a drift in $^{30}Si/^{28}Si$ of standard solutions of <1‰ over 60 h. It is corrected for by a standard-sample bracketing protocol. In order to minimise analytical blanks the dry aerosol is introduced to the plasma through a semi-demountable torch equipped with an alumina injector. Silicon isotope data are reported as deviations of $^{30}Si/^{28}Si$ and $^{29}Si/^{28}Si$ from the international standard NBS28 in parts per thousand (the standard delta notation $\delta^{30}Si$ and $\delta^{29}Si$, with X=30 or 29) as follows:

$$\delta^{X}\mathrm{Si} = \left[\frac{(^{X}\mathrm{Si}/^{28}\mathrm{Si})_{\mathrm{sam}} - (^{X}\mathrm{Si}/^{28}\mathrm{Si})_{\mathrm{NBS28}}}{(^{X}\mathrm{Si}/^{28}\mathrm{Si})_{\mathrm{NBS28}}}\right] \times 100$$

The long-term reproducibility of over 300 measurements of the IRMM-018 standard was ±0.14‰ ($2\sigma_{SD}$) for $\delta^{30}Si$ values and ±0.10‰ ($2\sigma_{SD}$) for $\delta^{29}Si$ values [38]. The standard data were acquired during 16 sessions between November 2004 and August 2005. Since all standards and samples were processed through the chemical separation procedure prior to each session this standard reproducibility also includes the repeatability of the applied chemical separation procedure. The silicon isotope composition of the river samples was reproducible during different measuring sessions with a similar average of 0.13‰ ($2\sigma_{SD}$) for $\delta^{30}Si$ and 0.08‰ ($2\sigma_{SD}$) for $\delta^{29}Si$. The precision given as *standard error of the mean* for over 12 duplicate analyses is thus limited to ±0.04‰ for $\delta^{30}Si$ values and ±0.03‰ for $\delta^{29}Si$ values at the 95% confidence level by our long-term reproducibility.

The sensitivity of the analytical setup varies but is typically ~10^{-10}A/ppm Si while running at high mass-resolution with an uptake rate of ~80 μl/min. Due to the very rapid washout performance of the DSN-100 the Si blank was reduced to below 2×10^{-13}A on mass ^{28}Si within 150 s of each measurement, which is equivalent to a ~1 ppb Si blank.

3. Results

3.1. Major element chemistry

The collected data, such as compositional long-term averages of the studied rivers and precipitation and the cation data for our samples are given in Tables 1 and 2, respectively. We used the long-term data in Table 1 to constrain major element chemistry. The examined rivers have total dissolved solid "TDS" concentrations (calculated as the sum of cation, anion and Si concentrations in ppm) ranging from 16 mg/l (Verzasca) to about 410 mg/l (Birs). In the Saane and Ticino the TDS was 330 and 180 mg/l, respectively. All rivers show strong seasonal gradients regarding the mean water temperature ranging between about 2 and 5 °C during the winter months (November to April) to ~14–17 °C during the summer months (May to October). The Verzasca, Ticino and the Saane have fairly stable pH values of 6.7, 7.8 and 8.2, respectively, with variations of 0.1–0.2 ($1\sigma_{SD}$). There is no long-term pH record for the Birs available but our measurements indicate lightly alkaline pH values around 8.2.

The rainwater contribution of major cations constitutes less than 5% of the riverine major cation fluxes of the Birs, Saane and Ticino. However, for the Verzasca, the estimated rainwater contribution is higher, between 5 and 14%. The input-corrected cation data of the collected samples were used to calculate a weathering flux (g/s), computed as the product of the measured discharge given in $m^3\ s^{-1}$ and the base cation concentration (sum of Ca^{2+}, Mg^{2+}, K^+ and Na^+ in mg/l).

On a molar basis, Ca^{2+} is the most abundant cation in most rivers; $[Ca^{2+}]>[Mg^{2+}]>[K^+Na^+]>[Si]$. The Verzasca shows a different composition of decreasing abundance: $[Ca^{2+}]>[Si]>[K^+Na^+]>[Mg^{2+}]$, documenting the importance of silicate-derived dissolved load in this river. The anionic species are dominated by $[HCO_3^-]>[SO_4^{2-}]>[Cl^-+NO_3^-]$. Noteworthy are high $[SO_4^{2-}]$ in the Ticino and Verzasca, and high $[NO_3^-]$ in the Verzasca (Fig. 2). The high $[SO_4^{2-}]$ is lithogenic, and is derived from the leaching of Mesozoic evaporites such as $CaSO_4$ that occur in the northern part of the Ticino valley [39]. An atmospheric origin is unlikely since both correction approaches do not eliminate the $[SO_4^{2-}]$ in these rivers. The high $[NO_3^-]$ in the Verzasca is probably derived from atmospheric inputs, as the Cl-approach eliminates this anomalous flux. Although Ticino and Verzasca drain the same gneissose lithology, the rivers show quite distinct chemical compositions, with a higher carbonate-derived component in the Ticino, based on higher Ca/Na and Mg/Na ratios [7]. Considering that all $[SO_4^{2-}]$ is derived from the dissolution of $CaSO_4$, the high Ca/Na ratios do overestimate the contribution from carbonate weathering. Assuming all SO_4^{2-} is derived from leaching of $CaSO_4$ the rainwater corrected riverine Ca^{2+} content can be calculated as follows:

$$Ca_{cor} = Ca^{*} - SO_4^{*} \times 0.42$$

Table 2
Discharge, compositional cation data (±2σ, not corrected for wet depositional input) and Si isotope data for each sample taken throughout 2004–2005

River	Sample	Discharge ±10% (m^3/s)	Ca^{2+} ±5%	Mg^{2+} ±4%	Na^{+} ±4% (mg/l)	K^{+}±4%	Si ±2%	Al^{3+} ±5% (μg/l)	$\delta^{30}Si$	95% SEM	$\delta^{29}Si$	95% SEM
									‰ (relative to NBS28)			
Birs	Mar 04	11.3	94.3	5.1	10.9	2.1	1.3	6	0.97	0.04	0.48	0.03
	May 04	8.0	91.3	5.1	8.4	2.3	1.8	3	0.61	0.04	0.34	0.03
	Aug 04	6.8	96.4	5.0	7.0	2.5	2.0	8	0.6	0.04	0.35	0.03
	Oct 04	4.1	93.7	5.8	10.0	3.3	1.8	45	0.79	0.04	0.4	0.03
	Jan 05	13.1	97.8	4.9	6.8	2.1	1.9	4	0.66	0.04	0.34	0.03
	Feb 05	11.3	100.7	5.3	14.8	2.2	1.9	6	0.62	0.04	0.35	0.03
	Mar 05	26.8	95.3	4.0	5.2	1.6	1.5	6	0.62	0.04	0.33	0.03
	May 05	15.2	94.3	4.8	6.1	1.9	1.5	5	0.73	0.04	0.36	0.03
	Jun 05	11.2	89.4	5.0	5.9	2.4	2.1	15	0.57	0.04	0.29	0.03
	Jul 05	6.5	98.7	5.2	7.7	2.5	2.2	9	0.78	0.04	0.4	0.03
Saane	Mar 04	37.3	81.8	8.2	9.1	1.9	1.8	6	0.97	0.04	0.54	0.03
	May 04	99.0	75.1	7.7	5.1	1.6	1.4	4	1.24	0.04	0.62	0.03
	Aug 04	89.9	65.6	7.1	4.6	1.4	1.5	3	0.68	0.04	0.37	0.03
	Oct 04	35.5	71.5	7.6	4.9	1.6	1.5	3	0.59	0.04	0.29	0.03
	Jan 05	33.9	84.2	9.7	9.7	2.2	1.9	3	1.13	0.04	0.59	0.03
	Feb 05	63.0	85.2	9.2	13.2	2.2	1.7	2	1.15	0.04	0.62	0.03
	Mar 05	62.7	87.2	9.2	11.7	2.1	1.5	3	1.16	0.04	0.66	0.03
	May 05	91.4	74.9	6.7	5.4	1.6	1.7	7	0.94	0.04	0.51	0.03
	Jun 05	51.0	70.7	6.2	4.3	1.3	1.7	5	0.78	0.04	0.43	0.03
	Jul 05	26.7	67.7	6.5	4.7	1.5	1.5	3	0.90	0.04	0.49	0.03
Ticino	Mar 04	31.3	55.5	10.2	1.8	1.6	1.4	14	0.96	0.04	0.48	0.03
	May 04	96.6	23.4	3.1	1.5	1.4	1.7	52	0.82	0.04	0.41	0.03
	Aug 04	112.1	37.8	5.4	2.0	2.1	2.1	28	0.73	0.04	0.39	0.03
	Oct 04	35.4	50.6	8.9	2.1	2.0	1.8	12	0.94	0.04	0.52	0.03
	Jan 05	33.9	50.5	9.3	1.6	1.7	1.9	7	0.86	0.04	0.45	0.03
	Feb 05	32.8	53.7	10.3	2.1	1.9	1.9	8	0.93	0.04	0.46	0.03
	Mar 05	34.7	48.2	8.3	1.9	1.9	1.8	9	1.09	0.04	0.55	0.03
	May 05	33.0	39.2	7.1	1.8	1.8	1.7	9	0.93	0.04	0.48	0.03
	Jun 05	88.2	34.4	5.1	1.7	1.6	1.7	19	0.89	0.04	0.46	0.03
	Jul 05	26.6	52.2	8.8	2.3	2.3	2.2	12	1.17	0.04	0.61	0.03
Verzasca	Mar 04	2.0	4.2	0.49	2.0	1.2	2.6	19	0.97	0.04	0.51	0.03
	May 04	29.2	2.1	0.25	0.7	0.6	1.4	65	0.53	0.04	0.25	0.03
	Aug 04	20.1	3.1	0.34	1.1	0.9	2.0	39	0.66	0.04	0.36	0.03
	Oct 04	2.9	3.5	0.42	1.5	1.4	2.6	11	0.80	0.04	0.44	0.03
	Jan 05	1.7	3.1	0.44	1.6	1.2	2.8	8	0.97	0.04	0.52	0.03
	Feb 05	0.8	3.7	0.50	1.7	1.2	2.9	6	1.01	0.04	0.54	0.03
	Mar 05	6.4	3.2	0.43	1.2	0.9	2.2	57	0.76	0.04	0.38	0.03
	May 05	5.5	3.2	0.37	1.0	0.8	2.1	33	0.74	0.04	0.38	0.03
	Jun 05	19.3	2.6	0.32	0.9	0.7	1.8	40	0.51	0.04	0.26	0.03
	Jul 05	2.4	3.5	0.42	1.4	1.1	2.5	17	0.99	0.04	0.47	0.03

Note that Ca* and SO_4^* are the measured riverine concentrations after correction for wet depositional input and 0.42 is the theoretical anhydrite $[Ca^{2+}]/[SO_4^{2-}]$ ratio. The anhydrite correction shows that nearly 70% of the dissolved $[Ca^{2+}]$ is contributed by evaporites. The associated Ca/Na ratios change from 16.9 to 5.3 after the anhydrite correction. The higher Mg/Na ratios of the Ticino can be related to dolomitic marbles that occur in the northern part of the Ticino valley. The larger catchment of the Ticino contains a larger diversity of different rocks, which are exposed to weathering and contribute to the dissolved load of the Ticino.

Birs and Saane have similar Ca/Na ratios (14.2± 5.4 and 16.6±4.1, respectively), indicating a carbonate-dominated chemistry [7]. According to the geological map [40] the catchment of the Saane also contains evaporites within the source area, so that the anhydrite correction should also be applied to correct the $[Ca^{2+}]$ concentration of the Saane. The correction shows that the dissolution of $CaSO_4$ might contribute up to 20% to the dissolved Ca load. The associated

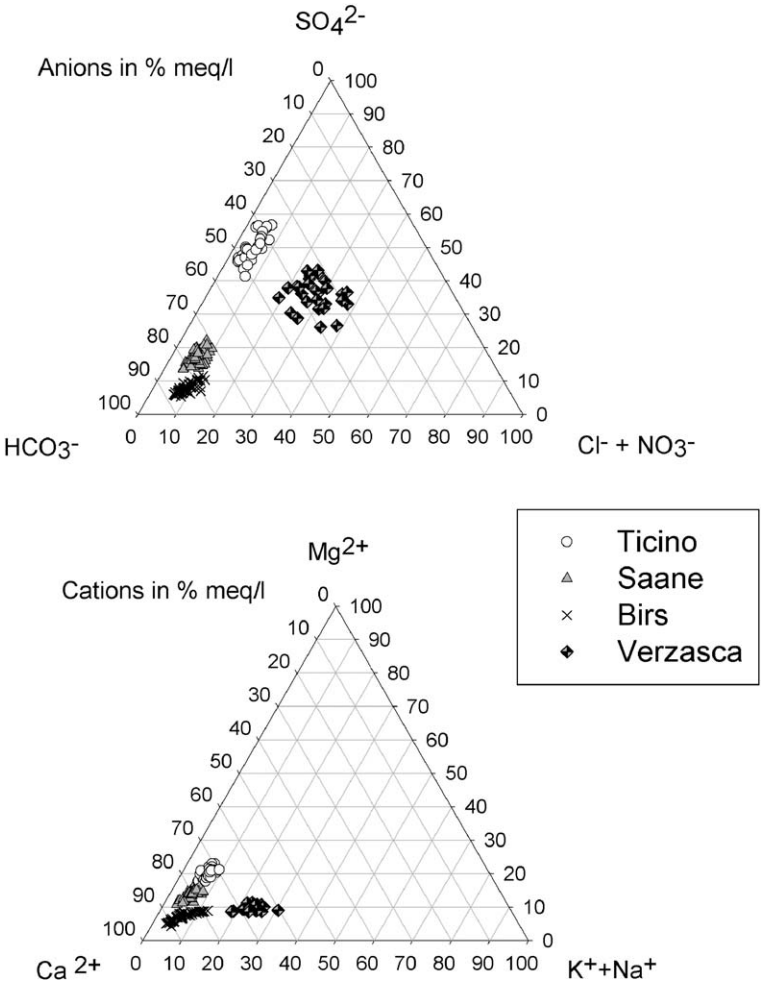

Fig. 2. Ternary diagrams showing the major cation and major anion composition of the studied rivers (uncorrected for wet depositional input and anhydrite contribution).

Ca/Na ratio changes to 13.2±3.6. The abundance of carbonate rocks within the catchment explains the overall carbonate-derived solute load within a mainly siliciclastic catchment. Although dolomites are exposed in the Swiss Jurassic Mountains, an average Mg/Na ratio of only 0.7 does not indicate significant contributions from dolomite weathering.

We used the long-term averages given in Table 1 and the software PhreeqC to calculate saturation states of the waters sampled here relative to primary and secondary minerals [41]. The calculation shows that all rivers are saturated with respect to kaolinite, thus this phase is one potential secondary mineral that might form within the catchment. Birs and Saane are saturated with respect to calcite but undersaturated with respect to quartz, reflecting the carbonate influence on the solute load. Ticino and Verzasca are undersaturated with respect to calcite and quartz. All rivers are undersaturated with respect to amorphous silica and primary silicates, such as anorthite, albite and K-feldspar.

3.2. Silicon concentrations and isotopic compositions

The measured Si isotope composition, the [Si] and cation concentration data and discharges for each sample are given in Table 2. All Si isotope measurements agree with the mass-dependent equilibrium fractionation line of Si, documenting the elimination of all molecular interferences ($\delta^{29}Si = 0.5178 \times \delta^{30}Si$, $R^2 = 0.96$), as shown in Fig. 3. All rivers carry a positive value of $\delta^{30}Si$ in the dissolved Si, consistent with previous conclusions that weathering and/or biological processes offset the composition of Si added to the oceans away from an average igneous $\delta^{30}Si$ range of

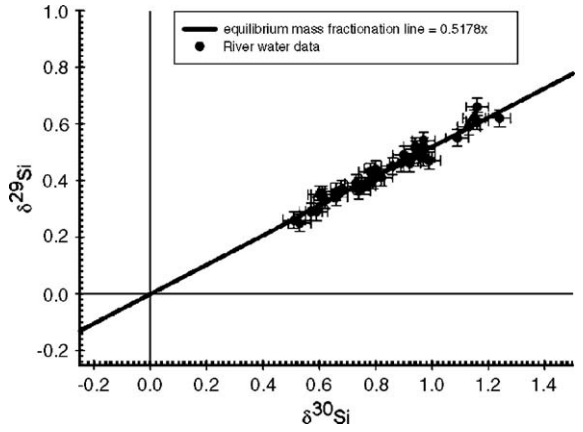

Fig. 3. Three-isotope plot showing that all river water samples follow the mass-dependent equilibrium fractionation array ($\delta^{29}Si = \delta^{30}Si \times 0.5178$) for Si.

−0.3 to 0.3‰ [18,42] toward heavy values [16,17]. The average δ^{30}Si of the Ticino (+0.93±0.12‰, $\pm 1\sigma_{SD}$) and the Saane (+0.95±0.22‰) are slightly heavier than the average of all data (+0.84±0.19‰); the average Birs composition is slightly lighter (+0.70±0.12‰) and Verzasca is similar (+0.79±0.19‰) to the mean Si isotope composition of all four rivers. A striking observation is the overall uniformity of these high precision data. Despite seasonal variations, the observed average Si isotope composition for each river is about the same and no systematic relationship exists between the Si isotopic composition of the river and the source lithology, TDS content or calculated weathering flux.

The high precision of the measurements facilitates the resolution of small seasonal variations in the Si isotope composition of the studied rivers (Table 2). Our results demonstrate for the first time that the Si isotope compositions of the rivers can undergo seasonal variations of 0.6‰ in δ^{30}Si (Fig. 4). Noteworthy is the seasonal co-variation between the δ^{30}Si and the [Si] of the Verzasca, which is not shown in the other three rivers (Fig. 4).

4. Discussion

In order to constrain the processes that control the Si isotope composition we assess the relationships between Si isotope variability, water chemistry and weathering flux.

4.1. Verzasca

For the mountainous Verzasca river the pronounced direct correlation between [Si] and Si isotope composition ($R^2 \sim 0.85$) over the sampling period (Fig. 5a) indicates a relatively simple process controlling the Si chemistry in these waters. A positive relationship between the concentration and isotopic composition of dissolved riverine Si was first recognised by De la Rocha et al. (2000) and interpreted as the result of enhanced weathering (yielding higher δ^{30}Si and higher [Si]) [17]. However, the total cation flux is dominated by the discharge (Fig. 5c) and actually *decreases* with Si isotopic composition (Fig. 5b (note log scale)). Therefore, the weathering flux is inversely related to the δ^{30}Si composition of the riverine dissolved Si.

The formation of clays is considered to be the key fractionation process during weathering. Clay formation should remove Al relative to Si, whilst leading to Si isotope fractionation, thus resulting fluids should have low Al/Si ratios correlated to high δ^{30}Si values, as shown to be the case in Fig. 5d. Given that clay formation is a key fractionation process, the upper intercept at ~+1‰ in Fig. 5d might represent a limit for clay-induced fractionation, reflecting exhaustion of the finite reservoirs of dissolved Al and the highest measured δ^{30}Si. The removal of Al during clay formation should dominate dissolved Si/Al ratios, and other cation to Al ratios, such as Ca/Al. This is exactly as observed for the Verzasca, and it is found that δ^{30}Si varies with Si/Al and Ca/Al (Fig. 6), implicating Si isotope fractionation during clay formation. However, processes dominated simply by clay formation cannot readily explain the observed co-variations between discharge, weathering flux and δ^{30}Si (Fig. 5b and c).

The speciation of Al in fresh water is considered to be either predominately dissolved as $Al(OH)_4^-$ [43] or associated in colloidal/particulate forms [44]. Therefore, elevated Al concentrations might reflect alumosilicate species (e.g. ultra-fine clays, <0.45 μm) or their leachates following acidification of the filtered samples. However, using the Al:Si ratios for clays of 1:2 and 1:1, the slope in Fig. 5d ($y = -11.74 \times +0.96$) would imply a δ^{30}Si value of the alumosilicate to be between −5‰ and −11‰. Such an extremely low δ^{30}Si value, given that the observed δ^{30}Si range for clays is between −2.3 and +0.1‰ [17,42], implies that the observed trend in Fig. 5d is not due to the incorporation of fine clay particles, and that Al is instead a truly dissolved and reactive species.

In order to explain the correlation between δ^{30}Si and discharge, the relationship between Si isotopic composition and water chemistry can more readily be interpreted in terms of mixing between two components (A and B), representing different solute pools with distinct Si isotopic and chemical compositions (Fig. 6).

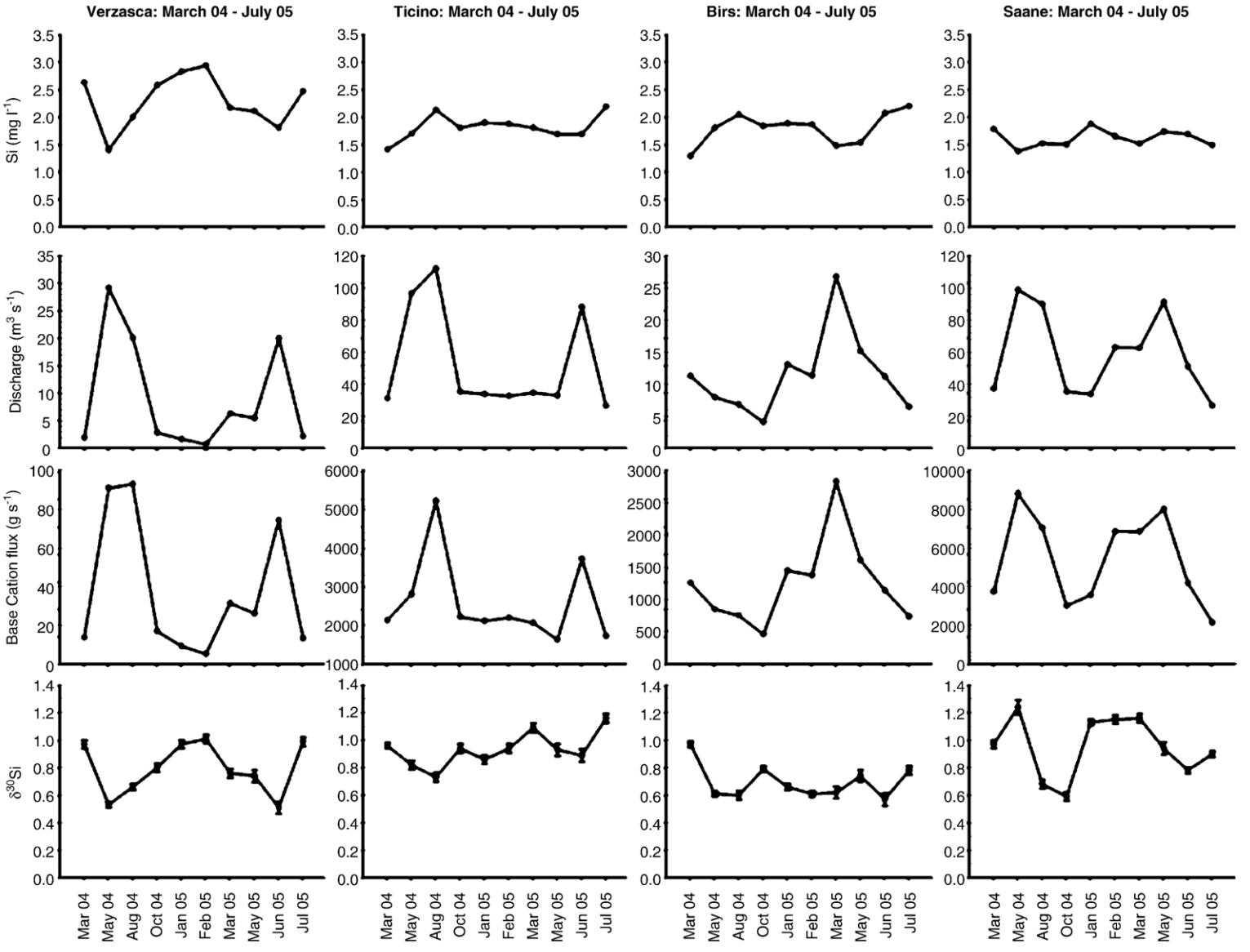

Fig. 4. Seasonal variations of measured Si concentration [Si], the discharge, base cation flux and δ^{30}Si for all rivers during the sampling period from March 2004 to July 2005. (Errors on δ^{30}Si are given as 95% SEM, errors on [Si] are 2%, errors on discharge and base cation flux ~10%.)

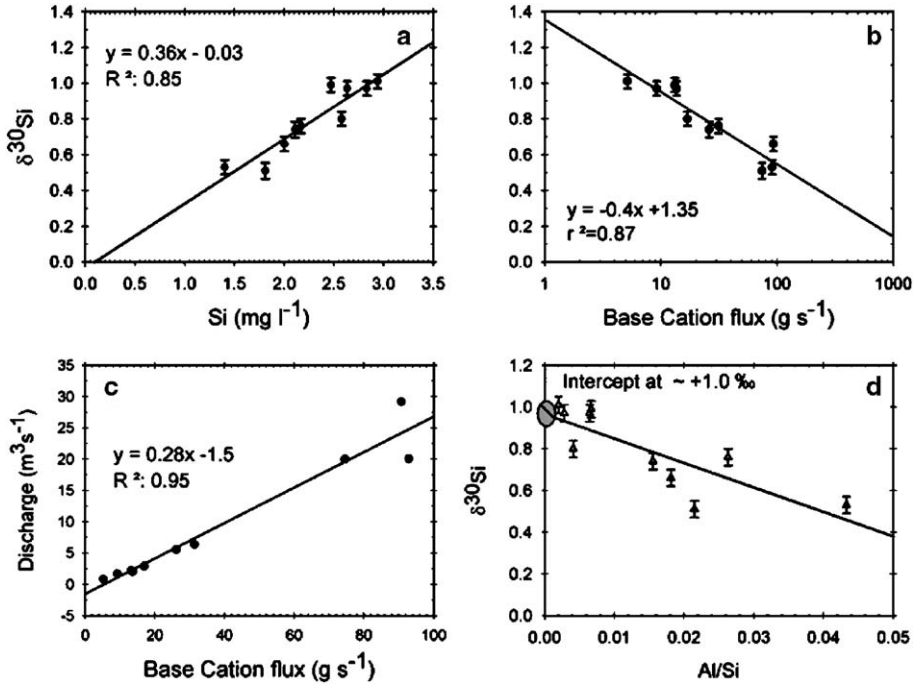

Fig. 5. Relationship between (a) δ^{30}Si and [Si], (b) δ^{30}Si and weathering flux (as base cation flux), (c) discharge and weathering flux and (d) δ^{30}Si and Al/Si ratios for the Verzasca. Uncertainties on δ^{30}Si ratios are given as 95% SEM, on discharge and fluxes are ~10%.

These two components can be used to characterise different facets of the weathering process. Component B, with the heaviest Si, low discharge and low solute fluxes, corresponds with low weathering fluxes, although the solute concentration is high. Clay formation appears active within the soil horizons and/or on in-situ sites within the host rock, as indicated by highly fractionated Si isotopes and the relative removal of Al. On this basis, Component B represents basal flow conditions, where the river discharge is mainly maintained through seepage from soil and/or ground waters. Component A is characterised by lower δ^{30}Si values, higher Al abundances and higher solute fluxes, indicating higher mineral dissolution rates and less effective clay formation. There are two potential sources of lighter Si isotopes and Al; (i) dissolution of clays and (ii) enhanced dissolution of primary silicates. The dissolution of clays is likely to contribute at least to some extent because the rainwater is undersaturated with respect to kaolinite and thus strong precipitation could cause clay dissolution. The enhanced solute flux reflected in the discharge would be consistent with this (Fig. 5c). The dissolution of both primary and secondary minerals releases Al and lighter Si isotopes into the river. This example shows that the Si isotope composition is inversely correlated with the silicate derived weathering flux, which is at its highest when the riverine δ^{30}Si is low.

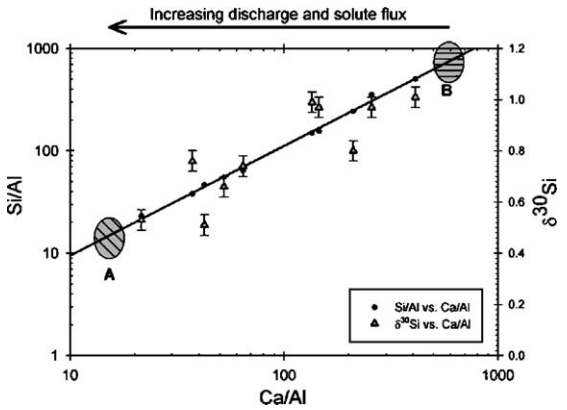

Fig. 6. The relationship of the δ^{30}Si composition and the water chemistry of the Verzasca can be described in a simple system using Si/Al vs. Ca/Al (black circles and line) and δ^{30}Si vs. Ca/Al (grey triangles). The system varies between two components A and B and is governed by the riverine discharge. Component B is likely to be basal flow; component A represents high superficial runoff.

The proposed association of component B with clay formation is consistent with previous work that has shown that δ^{30}Si of soil solutions and groundwater can be positive due to the dissolution of igneous minerals

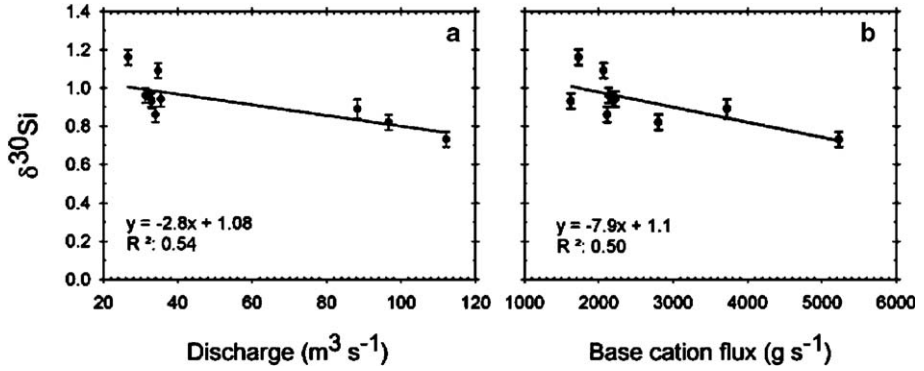

Fig. 7. Relationship between δ^{30}Si and (a) discharge and (b) base cation flux for the Ticino.

and the subsequent formation of secondary clay minerals [19,20]. It should be mentioned, however, that plants producing phytoliths utilise Al as well as Si and other macronutrients [45–50]. The related Si isotope fractionation and Al depletion might therefore be expected to be similar. However, estimates of Si/Al in phytoliths range from about 8–20 to 100–4000 (after [51]), and considering the sparse vegetation within the Verzasca valley, the biological uptake of Al should be negligible compared to the storage of Al in clays.

By excluding a significant biological storage of Si, the Si weathering flux thus corresponds to the chemical denudation rate of Si. Normalising the elemental flux to the catchment area, the chemical weathering of Si is on average about 2.9 t km^{-2} yr^{-1}, compared to an average base cation derived weathering flux of 6.3 t km^{-2} yr^{-1} which results in a total flux of 9.2 t km^{-2} yr^{-1}. This is about 5 times higher than the chemical denudation rate of other granitoid-dominated catchments in northern climates, but still lower than the chemical denudation rate of tropical granitoid catchments [8]. The silica weathering flux of ~6 t km^{-2} yr^{-1} is less than a value obtained for glaciated catchments within the Swiss Alps of ~10 t km^{-2} yr^{-1} [52].

4.2. Ticino

Although the Ticino drains a catchment lithology similar to the Verzasca, the basic water chemistry is quite different, apparently because of a contribution from carbonate and evaporite-derived weathering. There is no correlation between [Si] and Si isotope composition, but there are trends between Si isotope composition and discharge (R^2=0.54) and the base cation flux (R^2=0.51) (Fig. 7). The relationship is similar to the mixing trend of the Verzasca discussed above although not as pronounced, probably because of this additional complexity in dissolved source components (Fig. 8). Another important distinction between the Ticino and the Verzasca catchments is the presence of extensive soils and agriculture in the Ticino valley. Widespread, well-developed soils and agriculture provide extensive opportunities for Si to be biologically-utilised. The biological influence on the Si flux should thus be higher than in the Verzasca. The slightly higher average δ^{30}Si composition compared to the Verzasca would be consistent with this.

4.3. Birs and Saane

As with the Ticino, both the Birs and Saane do not show an overall correlation between [Si] and Si isotope composition. Again, the processes controlling the Si isotope composition within these rivers are complex. Neither river displays a relationship between Si isotope composition and discharge or weathering flux. It appears that the Si isotope composition is completely decoupled from the weathering flux in both rivers

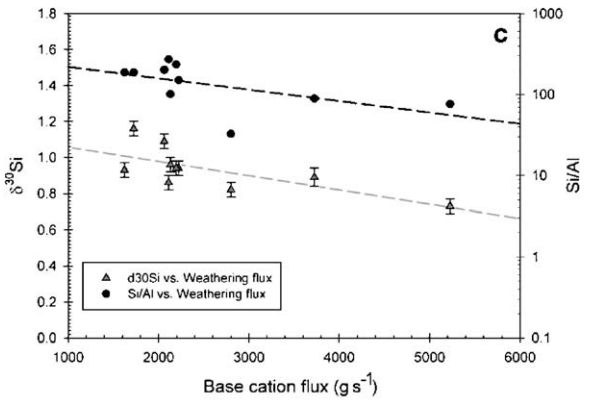

Fig. 8. The relationship between δ^{30}Si and base cation flux (grey triangle) and Si/Al ratios (black circles) for the Ticino.

because of the contributions from carbonate to the dissolved load.

The Si isotope composition of the Saane, however, shows a weak trend with Ca/Na ($R^2=0.33$) and Mg/Na ($R^2=0.35$) ratios, where lower δ^{30}Si values are related to higher Ca/Na and Mg/Na ratios and vice versa. The sample from May 2004 shows the highest δ^{30}Si composition among the entire data set and, considering a potential clay fractionation limit of ~+1‰ (see Section 4.1.) this value might be the result of biological fractionation. Excluding this sample improves the correlations between δ^{30}Si and Ca/Na and Mg/Na significantly ($R^2=0.70$ and 0.83, respectively) (Fig. 9a,b). As the catchment of the Saane is made up of silicate and carbonate rocks the correlation between Si isotope composition and Ca/Na and Mg/Na may indicate relative changes in the weathering intensity of both lithologies. The long-term dataset of the Saane shows that the Ca/Na ratio scales with the discharge (Fig. 9c), i.e. high discharge gives higher Ca/Na ratios. This relationship shows an enhanced release of Ca due to the favoured dissolution of highly soluble carbonates during high discharge periods. In fact, this means that the carbonate weathering rate is higher during high discharges. The Si isotope composition is, however, lower during this time, indicating an indirect relationship between Si isotope composition and discharge. As discussed in the previous sections, a lighter Si isotope composition is associated with an enhanced breakdown of silicate mineral phases and thus an increase in silicate weathering intensity. The changes in Ca/Na ratios with discharge result from an increase of carbonate weathering relative to silicate weathering during high discharge. The Si isotope composition decreases and thus also indicates an increase of primary silicate weathering. This is consistent with an increase of the total weathering (silicate+carbonate weathering) with discharge.

The carbonate-dominated Birs has the lowest average δ^{30}Si composition of all four studied rivers and the Ca/Na ratio also scales with discharge ($R^2=0.64$). The relation between δ^{30}Si and Ca/Na shows a similar trend, however, it is not as pronounced ($R^2=0.14$) as within the Saane. The weathering flux of the Birs is always dominated by carbonate dissolution and changes in weathering intensity do not influence Si isotope composition, which seems to be buffered by other processes. The [Si] of the Birs is not significantly lower than that of the other rivers, despite the fact that silicate rocks are of only minor importance. It has been

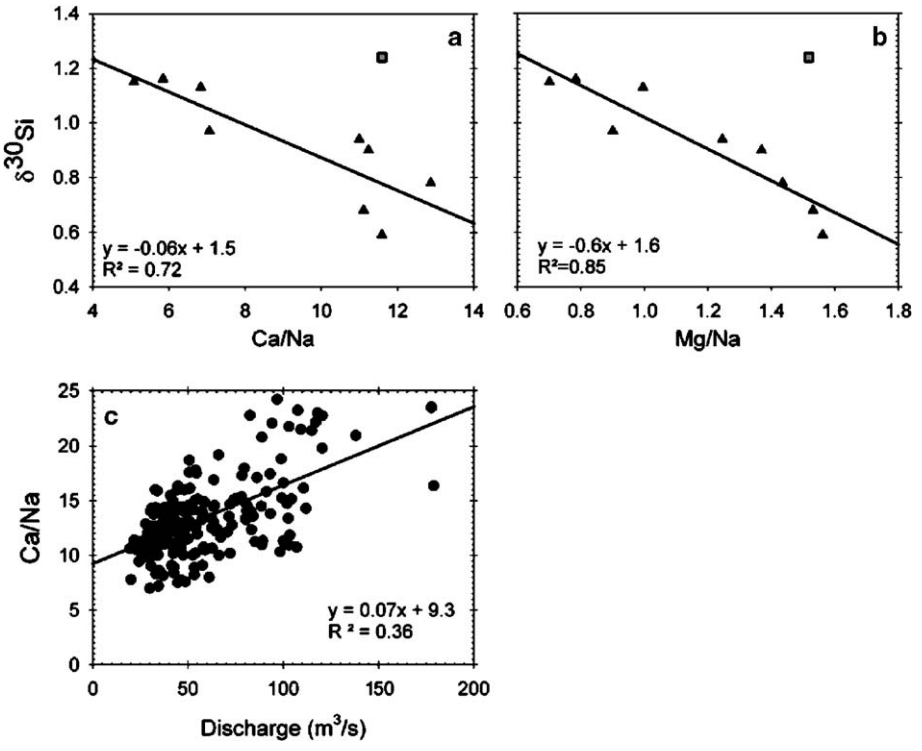

Fig. 9. Relationship between δ^{30}Si and (a) Ca/Na and (b) Mg/Na, excluding sample May 2004 (grey square), and between (c) discharge and Ca/Na for the Saane.

shown for forested catchments that the Si flux derived from the recycling of biogenic silica can be in excess of the weathering-derived Si flux [12,14,45,47,53]. Therefore, a biogenic origin for the Si in the Birs is plausible and consistent with the lower average δ^{30}Si, reflecting dissolution of lighter biogenic silica.

4.4. Implications for the global silicon budget

The average δ^{30}Si value of 40 samples from the Swiss rivers is +0.84±0.19‰ (±1σ_{SD}) and in good agreement with some previous studies [17,20]. No river-water studies yield δ^{30}Si values as high as +2.13± 0.74‰ reported for the Yangtze River in China [16], the reason for which is unclear. It has been suggested that stable continental shields with older and deeply weathered soils have lower average δ^{30}Si because of (i) weak present-day weathering and (ii) the dissolution of minerals that are mainly secondary in origin [20]. In contrast, tectonically-active mountain belts expose unaltered primary minerals and achieve high weathering rates leading to elevated δ^{30}Si in rivers. However, such models are not supported by the data presented here. Weathering regimes can be complex and many parameters, such as climate and topography, contribute to a regime that can be either (chemical) weathering-or transport-limited [54]. For example, if a watershed is weathering-limited due to its topography and climate (e.g. steep slopes, high precipitation), the soil formation is limited by intense physical erosion. Under these circumstances weathering favours the dissolution of highly soluble minerals, such as carbonates, silicate weathering is incomplete and the formation of soils and clays is limited due to high erosion rates. Under these conditions one would expect rivers to have generally low δ^{30}Si values due to ineffective clay induced fractionation. In turn, a transport limited watershed, where soil development and silicate weathering prevail should yield higher δ^{30}Si values in the water because of more clay formation, unless the main Si source is secondary in origin [20].

The high altitude watersheds of the Alps certainly represent weathering limited regimes [52], like the Verzasca valley, where the presence of steep slopes limits the development of soil by erosion [55]. Most of the Birs and Saane catchments have a low relief and in contrast to Verzasca soil formation prevails. The Si isotope composition of the studied alpine rivers is in good agreement with reported Si isotope compositions from transport-limited watersheds, e.g. Amazon and Congo river [17]. Our data indicate that the influence of different weathering regimes on the Si isotope composition is not as clear nor pronounced as previously proposed [20].

Despite the similarity in general tectonic environment between the European Alps and the Himalayas the results presented here are in stark contrast to the data recently reported for Chinese Rivers [16]. In both cases the effects should be dominated by a tectonically active mountain belt where fresh rock surfaces and young soils are exposed as a consequence of the last glaciation. Yet the Swiss rivers do not yield the extremely heavy δ^{30}Si values that are reported for the Chinese rivers. Based on the δ^{30}Si systematics of the Swiss rivers it seems to be unlikely that weathering of primary silicates and the formation of clays can produce dissolved riverine Si with δ^{30}Si values as high as +2.13‰. The δ^{30}Si of the Yangtze River is elevated where wetland and seasonally flooded rice fields start to appear [16], and it has been shown that the growth of rice plants is associated with a large Si isotope fractionation, and thus could account for the very high average δ^{30}Si of the Yangtze River [25]. However, recycling of organic matter from plants, which results in high biogenically-derived Si fluxes [12,14,45,47,53] should counterbalance the effect of biogenic Si isotope fractionation and limit δ^{30}Si to more normal values. Therefore, the reasons for these differences are unclear. It is however possible that there are systematic analytical offsets in reported δ^{30}Si values, as indicated by recent publications on the assessment of standard materials [38,56].

4.5. Glacial–interglacial variations in seawater δ^{30}Si

The seasonal δ^{30}Si variations reported here can be used to assess the impact on the global oceanic Si isotope composition of glacial–interglacial cycles. The sensitivity of the average Si isotope composition of the oceans has been recently addressed by De La Rocha

Table 3
Applying small offsets of ±0.2‰ to the riverine δ^{30}Si composition results in a significant shift of the continental δ^{30}Si input to the ocean

Riverine δ^{30}Si	Change in riverine δ^{30}Si	Initial Si Flux continental δ^{30}Si (in‰)	+10% Si Flux continental δ^{30}Si	−10% Si Flux continental δ^{30}Si
+1.0*	0.0*	+0.81*	+0.79*	+0.82*
+0.8	−0.2	+0.64	+0.65	+0.62
+1.2	+0.2	+0.98	+0.99	+0.95

The δ^{30}Si composition of the ocean is thus more sensitive to variations of the riverine δ^{30}Si composition than to changes of the riverine Si flux. *Data taken from [57].

and Bickle [57], who used a two box model with a constant δ^{30}Si value for the continental Si flux to the oceans of +0.8‰. This value represents a mass-balance between a 85% riverine input with an average δ^{30}Si of +1.0‰ and a 15% contribution of a non-riverine source with an average δ^{30}Si of −0.3‰ (after [2,58] in [57]). De La Rocha and Bickle argue that the Si flux must decrease by more than 50% of present day in order to change the input into the ocean significantly. However, the effects of glacial–interglacial changes in riverine δ^{30}Si are not considered. The average continental riverine discharge during the Last Glacial Maximum (LGM) was very similar to the present day value [59], as the global Si flux to the oceans would not have changed by a significant amount (~10%) compared to the present day value during glacial–interglacial cycles [60]. However, our results indicate that the δ^{30}Si composition of rivers can undergo large variations that relate to weathering style. Small offsets in average riverine δ^{30}Si from +1.0‰ to +1.2‰ and +0.8‰, result in the average continental input changing from +0.8‰ to +0.98‰ and +0.64‰, respectively (Table 3), and thus significantly change the Si isotopic input into the oceans. Extending the published mass-balance calculations [57] it is apparent that the average isotopic composition of dissolved continental Si that is transferred to the oceans is much more significant than changes in the total Si flux (Fig. 10). Variable continental δ^{30}Si inputs need to be considered in future applications of Si isotopes as a proxy for marine palaeoproductivity and past Si utilization.

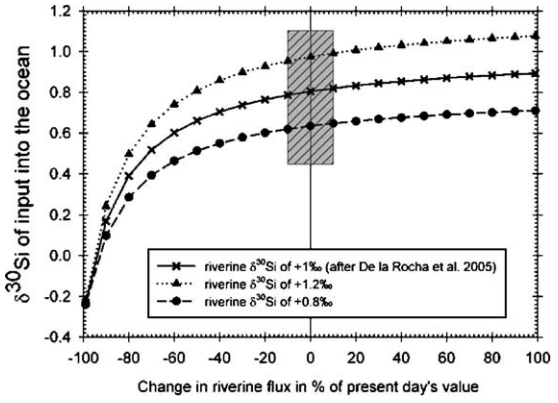

Fig. 10. Variations in the δ^{30}Si values of the continental input to the ocean due to variations in the riverine Si flux and the initial riverine δ^{30}Si composition. The model shows that the continental input into the oceans is more sensitive to changes in the riverine δ^{30}Si composition than to changes in the riverine Si flux. The grey box indicates changes in riverine Si flux of ±10%.

5. Conclusions

The average Si isotopic compositions of 4 Alpine rivers are very similar despite a range of weathering styles, climate, erosion flux and biomass. This is hard to reconcile with quite variable values reported for the Yangtze. However, the isotopic composition of dissolved Si varies significantly on a seasonal timescale with an amplitude of up to 0.6‰. Using variations in discharge, water chemistry and weathering flux the mechanisms controlling the sources of dissolved riverine Si can be constrained. The Si isotope composition of a high mountainous catchment reflects the mixing of soil/groundwater and high discharge waters originating from precipitation and snow melt. The underlying dominant mass fractionation process is the formation of clay, which incorporates lighter Si isotopes. The coupling between weathering flux and Si isotope composition implies that biological effects on dissolved Si are unimportant and can be neglected in high mountainous catchments. Catchments with higher proportions of carbonate rocks, cultivated soils and forests show a progressive decoupling of the Si isotope composition from the weathering flux. It appears to be common that an enhanced total weathering flux (carbonate+silicate weathering) is associated with lighter δ^{30}Si, even though carbonate dissolution dominates the solute load. The mechanisms controlling the Si isotope composition in lowland rivers are complex and cannot be distinguished unambiguously, but are likely a combination of Si derived from silicate weathering and recycling of biogenic silica. Overall, there appear to be regionally distinct mechanisms controlling the Si geochemical budget of river waters, namely; in high mountainous catchments Si is controlled by weathering of primary minerals and precipitation of clays, whilst is lowland areas the main control on the δ^{30}Si value and Si continental weathering flux may be biological utilization.

The continental input of Si into the oceans may have had variable δ^{30}Si values on short time-scales. Mass balance calculations show that the input into the ocean is more sensitive to variations of the riverine δ^{30}Si composition than to changes of the Si flux, and can lead to a change in the average δ^{30}Si value of the global ocean.

Acknowledgement

We wish to thank Jörg Rickli for fieldwork assistance, Urs Menet for a superb technical support, Felix Oberli, Andreas Süsli and Heiri Baur for technical

improvements of the Nu1700, and numerous other colleagues of the Isotope Group at IGMR for keeping the clean labs running. We would like to thank Sandra Steingruber for providing additional chemistry data for the Verzasca River and Ursi Schönenberger and Jürg Zobrist for providing additional data for the Saane River. We thank three anonymous reviewers for their insightful comments. This work was founded by the Swiss National Funds (Nr: 2000 20/101 780).

References

[1] K.L. Moulton, J. West, R.A. Berner, Solute flux and mineral mass balance approaches to the quantification of plant effects on silicate weathering, Am. J. Sci. 300 (2000) 539–570.

[2] P. Tréguer, D.M. Nelson, A.J. Van Bennekom, D.J. DeMaster, A. Leynaert, B. Quéguiner, The silica balance in the world ocean: a reestimate, Science 268 (1995) 375–379.

[3] J.C.J. Walker, P.B. Hays, J.F. Kasting, A negative feedback mechanism for the long term stabilization of the earth's surface temperature, J. Geophys. Res. 86 (1981) 9766–9782.

[4] R.A. Berner, A.C. Lasaga, R.M. Garrels, The Carbonate-silicate geochemical cycle and it's effect on atmospheric carbon dioxide over the past 100 million years, Am. J. Sci. 283 (1983) 641–683.

[5] G.J. Bluth, L.R. Kump, Lithologic and climatologic controls of river chemistry, Geochim. Cosmochim. Acta 58 (1994) 2341–2359.

[6] Y. Huh, J.M. Edmond, The fluvial geochemistry of the rivers of eastern Siberia: III. Tributaries of the Lena and Anabar draining the basement terrain of the Siberian craton and the Trans-Baikal highlands, Geochim. Cosmochim. Acta 63 (1999) 967–987.

[7] J. Gaillardet, B. Dupre, P. Louvat, C.J. Allegre, Global silicate weathering and CO2 consumption rates deduced from the chemistry of large rivers, Chem. Geol. 159 (1999) 3–30.

[8] R. Millot, J. Gaillardet, B. Dupre, C.J. Allegre, The global control of silicate weathering rates and the coupling with physical erosion: new insights from rivers of the Canadian Shield, Earth Planet. Sci. Lett. 196 (2002) 83–98.

[9] M.E. Raymo, W.F. Ruddiman, P.N. Froelich, Influence of the late Cenozoic mountain building on the ocean geochemical cycles, Geology 16 (1988) 649–653.

[10] Y. Huh, L.H. Chan, J.M. Edmond, Lithium isotopes as a probe of weathering processes: Orinoco river, Earth Planet. Sci. Lett. 194 (2001) 189–199.

[11] J.S. Pistiner, G.M. Henderson, Lithium-isotope fractionation during continental weathering processes, Earth Planet. Sci. Lett. 214 (2003) 327–339.

[12] A. Alexandre, J.D. Meunier, F. Colin, J.M. Koud, Plant impact on the biogeochemical cycle of silicon and related weathering processes, Geochim. Cosmochim. Acta 61 (1997) 677–682.

[13] J.D. Meunier, F. Colin, C. Alarcon, Biogenic silica storage in soils, Geology 27 (1999) 835–838.

[14] V.C. Farmer, E. Delbos, J.D. Miller, The role of phytolith formation and dissolution controlling concentration of silica in soil solutions and streams, Geoderma 127 (2005) 71–79.

[15] A.N. Halliday, C.H. Stirling, P.A. Freedman, F. Oberli, B.C. Reynolds and R.B. Georg, in press. High precision isotope ratio measurements using multiple collector inductively coupled plasma mass spectrometry., Encyclopedia of Mass Spectrometry 5, pp. Chapter 17.

[16] T. Ding, D. Wan, C. Wang, F. Zhang, Silicon isotope compositions of dissolved silicon and suspendet matter in the Yangtze river, China, Geochim. Cosmochim. Acta 68 (2004) 205–216.

[17] C.L. De La Rocha, M.A. Brzezinski, M.J. DeNiro, A first look at the distribution of the stable isotopes of silicon in natural waters, Geochim. Cosmochim. Acta 64 (2000) 2467–2477.

[18] C.B. Douthitt, The geochemistry of the stable isotopes of silicon, Geochim. Cosmochim. Acta 46 (1982) 1449–1458.

[19] R.B. Georg, B.C. Reynolds, A.N. Halliday, C. Zhu, Fractionation of stable Si isotopes during in-situ dissolution of feldspars and formation of secondary clay minerals, EOS Trans. AGU Fall Meet. Suppl. 86 (2005) (Abstract).

[20] K. Ziegler, O.A. Chadwick, M.A. Brzezinski, E.F. Kelly, Natural variations of δ^{30}Si ratios during progressive basalt weathering, Hawaiian Islands, Geochim. Cosmochim. Acta 69 (2005) 4597–4610.

[21] K. Ziegler, O.A. Chadwick, A.F. White, M.A. Brzezinski, δ^{30}Si systematics in a granitic saprolite, Puerto Rico, Geology 33 (2005) 817–820.

[22] C.L. De La Rocha, M.A. Brzezinski, M.J. DeNiro, Fractionation of silicon isotopes by marine diatoms during biogenic silica formation, Geochim. Cosmochim. Acta 61 (1997) 5051–5056.

[23] C.L. De La Rocha, M.A. Brzezinski, M.J. DeNiro, A. Shemesh, Silicon-isotope composition of diatoms as an indicator of past oceanic change, Nature 395 (1998) 680–683.

[24] T. Ding, D. Wan, C. Wang, F. Zhang, Large and systematic silicon isotope fractionation discovered in single sticks of bamboo, Geochim. Cosmochim. Acta 67 (Suppl. 1) (2003) A79.

[25] T. Ding, G.R. Ma, M.X. Shui, D.F. Wan, R.H. Li, Silicon isotope study on rice plants from the Zhejiang province, China, Chem. Geol. 218 (2005) 41–50.

[26] D.E. Varela, C.J. Pride, M.A. Brzezinski, Biological fractionation of silicon isotopes in Southern Ocean surface waters, Glob. Biogeochem. Cycles 18 (GB1047) (2004) 1–8.

[27] B.C. Reynolds, M. Frank, A.N. Halliday, Silicon isotope fractionation during nutrient utilization in the North Pacific, Earth Planet. Sci. Lett. 244 (2006) 431–443.

[28] S. Opfergelt, D. Cardinal, C. Henriet, L. Andre, B. Delvaux, Silicon isotope fractionation between plant parts in banana: in situ vs. in vitro, J. Geochem. Explor. 88 (2006) 224–227.

[29] Wenger, C., Steiger, R., 1990. Karte der Vorkommen mineralischer Rohstoffe der Schweiz, Blatt 1 Tessin-Uri/Carta delle materie prime minerali della Svizzera, Foglio 1 Ticino-Uri, 1:200 000, Schweizerische Geotechnische Kommission.

[30] K. Grasshoff, On the determination of silica in sea water, Deep-Sea Res. 11 (1964) 597–604.

[31] E. Binderheim-Bankay, A. Jakob, P. Liechti, NADUF — Messresultate 1977–1998, Federal Office for the Environment (FOEN), Bern, 2000, p. 241.

[32] NABEL — Luftbelastung 2004, pp. 217, Federal Office for the Environment (FOEN) and Swiss Institute Material Sciences and Technology (EMPA), Berne, 2005.

[33] R.F. Stallard, J.M. Edmond, Geochemistry of the Amazon: 1. Precipitation chemistry and the contribution to the dissolved load at the time of peak discharge, J. Geophy. Res. NO C10 86 (1981) 9844–9858.

[34] R.G. Darmody, C.E. Thorn, R.L. Harder, J.P.L. Schlyter, J.C. Dixon, Weathering implications of water chemistry in artic–alpine environment, northern Sweden, Geomorphology 34 (2000) 89–100.

[35] R.B. Georg, B.C. Reynolds, M. Frank, A.N. Halliday, New sample preparation techniques for the precise determination of

the Si isotope composition of natural samples using MC-ICP-MS, Chem. Geol. (in press).
[36] C.L. De La Rocha, Measurement of silicon stable isotope natural abundances via multicollector inductively coupled plasma mass spectrometry (MC-ICP-MS), Geochem. Geophys. Geosyst. 3 (2002) (art. no.— 1045).
[37] D. Cardinal, L.Y. Alleman, J. de Jong, K. Ziegler, L. Andre, Isotopic composition of silicon measured by multicollector plasma source mass spectrometry in dry plasma mode, J. Anal. At. Spectrom. 18 (2003) 213–218.
[38] B.C. Reynolds, R.B. Georg, F. Oberli, U.H. Wiechert, A.N. Halliday, Re-assessment of silicon isotope reference materials using high-resolution multi-collector ICP-MS, J. Anal. At. Spectrom. 21 (2006) 266–269.
[39] S. Pastorelli, L. Marini, J. Hunziker, Chemistry, isotope values (δD, $\delta^{18}O$, $d^{34}S_{SO4}$) and temperatures of the water inflows in two Gotthardt tunnels, Swiss Alps, Appl. Geochem. 16 (2001) 633–649.
[40] D. Cavalli, E.G. Haldemann, R. Kündig, D. Reber, J.D. Rouiller, M. Schafer, 1998. Karte der Vorkommen mineralischer Rohstoffe der Schweiz, Blatt 2 Wallis-Berner Oberland/Carte des matières premières minérales de la Suisse, Feuille 2 Valais-Oberland bernois, 1:200 000, Schweizerische Geotechnische Kommission.
[41] D.L. Parkhurst, C.A.J. Appelo, User's guide to PHREEQC (Version2) — A Computer Program for Speciation, Batch-reaction, One-dimensional Transport and Inverse Geochemical Calculations, 1999, 310 pp.
[42] T. Ding, S. Jiang, D. Wan, Y. Li, H. Song, Z. Liu, X. Yao, Silicon Isotope Geochemistry, Geological Publishing House, Beijing, China, 1996.
[43] N.M. Hassan, J.D. Murimboh, A.L.R. Sekaly, R. Mandal, C.L. Chakrabarti, D.C. Grégoire, Cascade ultrafiltration and competing ligant exchange for kinetic speciation of aluminium, iron, and nickel in fresh water, Anal. Bioanal. Chem. 384 (2006) 1558–1566.
[44] S. Upadhyay, P.S. Liss, T.D. Jickells, Sorption model for dissolved aluminium in freshwaters, Aquat. Geochem. 8 (2002) 255–275.
[45] A.L. Carnelli, M. Madella, J.P. Theurillat, Biogenic silica production in selected Alpine plant species and plant communities, Ann. Bot. 87 (2001) 425–434.
[46] A.L. Carnelli, M. Madella, J.P. Theurillat, B. Ammann, Aluminum in the opal silica reticule of phytoliths: a new tool in palaeoecological studies, Am. J. Bot. 89 (2002) 346–351.
[47] A.L. Carnelli, J.P. Theurillat, M. Madella, Pytholith types and type-frequencies in subalpine–alpine plant species of the European Alps, Rev. Palaeobot. Palynol. 129 (2004) 39–65.
[48] F. Bartoli, L.P. Wilding, Dissolution of biogenic opal as a function of its physical and chemical properties, Soil Sci. Soc. Am. J. 44 (1980) 873–878.
[49] R.A.J. Wüst, R.M. Bustin, Opaline and Al–Si phytoliths from a tropical mire system of West Malaysia: abundance, habit, elemental composition, preservation and significance, Chem. Geol. 200 (2003) 267–292.
[50] M.J. Hodson, A.G. Sangster, Aluminum/silicon interactions in conifers, J. Inorg. Biochem. 76 (1999) 89–98.
[51] F. Bartoli, Crystallochemistry and surface properties of biogenic silica, J. Soil Sci. 36 (1985) 335–350.
[52] A.J. West, A. Galy, M. Bickel, Tectonic and climatic controls on silicate weathering, Earth Planet. Sci. Lett. 235 (2005) 211–228.
[53] D.J. Conley, Terestrial ecosystems and the global biogeochemical silica cycle, Glob. Biogeochem. Cycles 16 (2002) 681–688.
[54] A. Jacobson, J. Blum, C.P. Chamberlain, D. Craw, P.O. Koons, Climatic and tectonic controls on chemical weathering in the New Zealand Southern Alps, Geochim. Cosmochim. Acta 67 (2003) 29–46.
[55] J.I. Drever, J. Zobrist, Chemical weathering of silicate rocks as a function of elevation in the southern Swiss Alps, Geochim. Cosmochim. Acta 56 (1992) 3209–3216.
[56] T. Ding, D. Wan, R. Bai, Z. Zhang, Y. Shen, R. Meng, Silicon isotope abundance ratios and atomic wights of NBS-28 and other reference materials, Geochim. Cosmochim. Acta 69 (2005) 5487–5494.
[57] C.L. De La Rocha, M.J. Bickle, Sensitivity of silicon isotopes to whole-ocean changes in the silica cycle, Mar. Geol. 217 (2005) 267–282.
[58] H. Elderfield, A. Schultz, Mid-ocean ridge hydrothermal fluxes and the chemical composition of the ocean, Annu. Rev. Earth Planet. Sci. 24 (1996) 191–224.
[59] G. Munhoven, Glacial–interglacial changes of continental weathering: estimates of the related CO_2 and HCO_3^- flux variations and their uncertainties, Glob. Planet. Change 33 (2002) 155–176.
[60] I.W. Jones, G. Munhoven, M. Tranter, P. Huybrechts, M.J. Sharp, Modelled glacial and non-glacial HCO_3, Si and Ge fluxes since the LGM: little potential for impact on atmospheric CO_2 concentrations and a potential proxy of continental chemical erosion, the marine Ge/Si ratio, Glob. Planet. Change 33 (2002) 139–153.